IEEE Transactions on Reliability, 53 **(4) (Dec. 2004), pp. 542-550**

Bounding the Times to Failure of 2-Component Systems

Daniel Berleant and Jianzhong Zhang
Department of Electrical and Computer Engineering
Iowa State University
Ames, Iowa 50014

Index Terms **– Uncertainty quantification, model uncertainty, Cdf envelopes, DEnv, dependency bounds, functions of random variables.**

Abstract

Characterizing the distribution of times to failure in 2-component systems is an important special case of a more general problem, finding the distribution of a function of random variables. Advances in this area are relevant to reliability as well as other fields, and influential papers on the topic have appeared in the reliability field over a span of many years. Using failure times of 2-component systems as a vehicle, this report begins by reviewing a technique for characterizing distributions of functions of random variables when the dependency relationship between the random variables used as inputs to the function is unknown. The technique addressed is called Distribution Envelope determination (DEnv). Using this review as a foundation, an extension to DEnv is described which applies to cases where means and variances of the input distributions are known, and *partial* information about dependency is available in the form of a value for correlation. Pearson correlation is used because it is the most commonly encountered correlation measure. This reason is important because the assumption of independence, while common, is frequently problematic. Yet the opposite extreme of no assumption about dependency may mean ignoring available information which could affect the analysis.

Acronyms[1]

Cdf	Cumulative distribution function
pdf	Probability density function
DEnv	Distribution Envelope Determination algorithm

Notation

$F_k(t)$	Cumulative probability of failure for component C_k
$f_k(t)$	Probability density function describing failure for component C_k
$[l, h]$	Interval with lower bound l and upper bound h, inclusive of the end points

1 Introduction

We consider the problems of determining the time until the first of two components fails, and the time until both fail. These problems can be addressed by modeling the time to failure of each component with a probability density function (pdf). The area under the pdf, over a given time interval, is the probability of failure during that time interval.

If a joint density function can be obtained, each point in it could be labeled with a time t whose value is the minimum of its two marginal values if we wish to characterize the time of first component failure, or the maximum to characterize the time to failure of both components. Integrating the joint density from 0 to t produces a cumulative probability of failure as a function of t. Alternatively, the two marginals could be integrated to get their corresponding cumulative distribution functions $F_1(t)$, and $F_2(t)$. Assuming *s*-independence, the probability of both components failing by time t is $F_1(t)F_2(t)$. The probability of the first component failure occurring by time t may be

[1] The singular and plural of an acronym are always spelled the same.

stated using different, but algebraically equal expressions depending on the motivating intuition:

$$\begin{aligned} & 1-(1-F_1(t))(1-F_2(t)) \\ & = F_1(t)+F_2(t)-F_1(t)F_2(t) \\ & = F_1(t)(1-F_2(t))+F_2(t)(1-F_1(t))+F_1(t)F_2(t). \end{aligned}$$

The assumption of s-independence in the foregoing analysis is a serious limitation. Often other dependency relationships hold among events, motivating methods for calculation which take known dependencies into account (see Section 2.1; also [19]; additional references in [21]). Reliability modeling with the wrong dependency relationship can lead to decisions which are much more expensive than necessary [6], yet the actual dependency relationship may be unclear. Thus, explicitly accounting for the degree [10] of such model uncertainty can lead to understanding (i) the range of possibly optimal decisions, and (ii) the potential value of knowing the correct dependency model.

The following four examples illustrate the variety and pervasiveness of situations relevant to reliability engineering in which the dependency relationship between two random variables, in the present case times to failure, is unknown.

Example 1 – lights. Consider rooms at a conference center. Each room has two lights. The switch for one light is by one entrance, and the switch for the other is at the other entrance. Users who like plenty of light will turn on both lights, while others will turn on only the one at the entrance from which they enter the room. A user tends to repeatedly use the same conference rooms, so each room has its own light usage profile.

Based on past experience, the engineer has determined a distribution function describing, for the conference center as a whole, the amount of time a light operates before it needs a new bulb or other service. We wish to characterize the distribution

describing the time until either of the lights in a given conference room will need service. Similarly, we wish to characterize the distribution describing the time until both lights have failed in a given conference room (thereby rendering the room unusable until repaired).

The distributions for the times to failure of the lights in a room might be *s*-independent. Alternatively they might be positively correlated if, for example, users of the room tend to prefer bright lighting and so use both lights at once, causing both to wear simultaneously. On the other hand, the distributions might be negatively correlated. For example, users of a room may tend to use only one light, so when one light is on and undergoing wear, the other is probably off and not undergoing wear. If users tend to enter the room by one of its entrances in preference to the other, one light will tend to last less time than average, and the other more time.

Example 2 – tires. A car has two new Flamerock brand tires installed. These tires are rated for 30,000 miles, but their actual lives are samples of a distribution function which expresses variations in duty conditions, the chance of failure due to damage, manufacturing variations, etc. The company is offering a special replacement warranty for customers installing two new tires. Understanding the cost of offering the warranty requires characterizing the distribution describing the distance traveled before either tire requires replacement, as well as before both will require replacement.

As in the previous example, the distributions of the tire lifetimes (in miles) might not be *s*-independent. They would be positively correlated if tire life for a given customer is dominated by such factors as the type of road surface typically traveled, or poor maintenance of tire pressure. On the other hand, they would be negatively correlated if

tire life is dominated by the fact that a customer has installed one on the heavier front of the (front wheel drive) vehicle and one on the lighter rear, and does not rotate tires, so that the front tire wears faster than average and the rear, slower.

Example 3 – keyboard and mouse. A computer is equipped with keyboard and mouse. Given a distribution for the life of each, what is the time until one of them fails? The individual distributions for time to failure might be *s*-independent. Or, they might be positively correlated, as in a harsh environment which tends to wear out both components sooner than expected, or in a low use environment in which both tend to last longer than expected. The lifetimes might also be negatively correlated, as for a user who mostly types, thus wearing the keyboard and preserving the mouse; or a user who mostly points and clicks, thus wearing the mouse and preserving the keyboard.

Example 4 – electric generators. Two electric generators are producing power. Distributions are known which describe the time to failure of each, and it is desired to characterize the time to the first failure. The times to failure of the individual generators could be correlated positively, or negatively. They would be correlated positively if both are usually operated at the same production level, because production level is a predictor of time to failure. They would be correlated negatively if power is generated preferentially from one generator, as would occur when one produces electricity at lower cost than the other. The higher production from one generator would cause it to wear while preserving the other.

1.1 Solution Approach

Because the dependency relationships in the previous problems are unknown, the joint probability density functions are underdetermined. Thus the distributions for the times to

failure of one component, and of both, are also underdetermined. While any specific dependency relationship is associated with some specific result distribution, we wish to avoid specifying a particular dependency relationship when there is insufficient evidence to justify one. In that case, the problem is underspecified, and a solution could do no better than to describe the set of possible distributions for the solution. Left and right envelopes can specify bounding curves within which the trajectory of any Cdf in the set must lie (see Figure 1; also [9], [13]).

For determining the left and right envelopes, an analytical approach is one strategy. This imposes limitations on the form of the input distributions. Monte Carlo simulation is an alternative. However, this leads to envelopes which are not crisply described, and tends to handle tails problematically [12]. A numerical approach is another strategy in which the input distributions need not be described with any particular type of equation or even with equations at all. A numerical solution does however involve discretization, and consequently the possibility of imperfect representation of the inputs. For many numerical methods, the result is error in the output. However, the numerical method described here converts discretization error in the inputs into increased separation of the envelopes instead.

One numerical algorithm for deriving such envelopes, Probabilistic Arithmetic, is based on copulas [13] [17]. It was developed into a numerical algorithm by Williamson and Downs [20], and is implemented in a commercial software package targeted at the mathematical ecology area, although the tool itself, RiskCalc, is not domain specific [11]. Another algorithm, Distribution Envelope Determination (DEnv), uses intervals as well

as minimal and maximal cumulations consistent with the set of possible joint density functions [5]. It is implemented in a program called Statool.

The algorithms have important underlying similarities [18], as well as pragmatic and theoretical differences [2]. One pragmatic difference is that DEnv and its implementation in Statool do not use copulas, making it more accessible to individuals not already familiar with copulas. Another pragmatic difference is that RiskCalc incorporates handling of other forms of uncertainty, in particular fuzzy numbers and hybrid numbers, while Statool is limited to the domain of distributions.

Theoretical differences arise from the fact that RiskCalc uses copulas while Statool does not. Because copulas normalize the marginals by stretching them into a standard shape [17], computations which rely on the un-normalized curves will be problematic in copula-based algorithms. Pearson (product-moment) correlation, the kind generally meant by use of the term "correlation" but by no means the only kind, is an important example. Thus, while Statool incorporates Pearson correlation, it is unclear how copula-based methods could. On the other hand, Spearman rank correlation is an example of a type of correlation which is natural to apply to normalized marginals. More generally, copulas are a mathematically elegant vehicle for describing a wide variety of constraints on dependency, though not Pearson correlation.

In the next section, the DEnv algorithm is explained. An explanation of DEnv in the context of a reliability problem is new in the present report. Also new is an explanation of correlation (Section 2.3) in the important case where the means & variances of the times to failure, and the value of the Pearson correlation coefficient, are available.

2 Distribution Envelope Determination (DEnv)

The DEnv algorithm works with the set of joint density functions which are possible for given marginals. In the context of the example problems described in the Introduction, a marginal pdf models the time to failure of a light, a tire, a keyboard, a mouse, or an electric generator. The joint density function of two marginals (one for each of two components C_1 & C_2) assigns a probability density $f(t_1,t_2)$ to each point (t_1,t_2) for which t_1 is a failure time for component C_1, and t_2 is a failure time for C_2.

Each point (t_1,t_2) in a joint density function can have another value associated with it besides a probability density. If that value is $t_{\min}=\min(t_1,t_2)$, then $F_{one}(t) = \int_{t_1} \int_{t_2|t_{\min} \le t} f(t_1,t_2)dt_1dt_2$ gives the probability that the first component to fail does so by time t. Similarly, if that value is $t_{\max}=\max(t_1,t_2)$, then $F_{both}(t) = \int_{t_1} \int_{t_2|t_{\max} \le t} f(t_1,t_2)dt_1dt_2$ gives the probability that both components will fail by time t.

Let set S be the set of joint density functions consistent with the marginals. Let joint density function f be termed *extremal* for time t and function F_{one} if it leads to a higher or lower value for $F_{one}(t)$ than any other f in S. Similarly, f may be extremal for time t and F_{both}. DEnv finds joint density functions which are extremal. Finding extremal joint density functions for appropriate values of t makes it possible to plot envelopes for F_{one} or F_{both} (Figure 1). The DEnv technique computes these envelopes using discrete representations of the marginals and joint density functions. A step by step description follows.

1) The probability density function (pdf) for each component's time to failure is discretized using a histogram-like representation, consisting of a set of intervals, and an associated probability for each interval. Figure 2 illustrates this process. Although only four density functions consistent with the discretization are shown in the Figure, an infinite number of others are as well. The flat tops of the histogram bars are merely a graphical convenience, because the details of the distribution of a bar's probability over the interval it spans are actually unconstrained. Discretizations can also be represented numerically, as in the leftmost column & the bottom row of Table 1.

[30.0,100.0] ***p*=0.031**	t_f=[0,5.0] t_s=[30.0,100.0] p_{16}=0.0031	t_f=[5.0,8.0] t_s=[30.0,100.0] p_{26}=0.0031	t_f=[8.0,10.0] t_s=[30.0,100.0] p_{36}=0.0093	t_f=[10.0,12.0] t_s=[30.0,100.0] p_{46}=0.0093	t_f=[12.0,20.0] t_s=[30.0,100.0] p_{56}=0.0031	t_f=[20.0,80.0] t_s=[30.0,100.0] p_{66}=0.0031
[24.0,30.0] ***p*=0.031**	t_f=[0,5.0] t_s=[24.0,30.0] p_{15}=0.0031	t_f=[5.0,8.0] t_s=[24.0,30.0] p_{25}=0.0031	t_f=[8.0,10.0] t_s=[24.0,30.0] p_{35}=0.0093	t_f=[10.0,12.0] t_s=[24.0,30.0] p_{45}=0.0093	t_f=[12.0,20.0] t_s=[24.0,30.0] p_{55}=0.0031	t_f=[20.0,30.0] t_s=[24.0,80.0] p_{65}=0.0031
[18.0,24.0] ***p*=0.063**	t_f=[0,5.0] t_s=[18.0,24.0] p_{14}=0.0063	t_f=[5.0,8.0] t_s=[18.0,24.0] p_{24}=0.0063	t_f=[8.0,10.0] t_s=[18.0,24.0] p_{34}=0.0189	t_f=[10.0,12.0] t_s=[18.0,24.0] p_{44}=0.0189	t_f=[12.0,20.0] t_s=[18.0,24.0] p_{54}=0.0063	t_f=[18.0,24.0] t_s=[20.0,80.0] p_{64}=0.0063
[12.0,18.0] ***p*=0.125**	t_f=[0,5.0] t_s=[12.0,18.0] p_{13}=0.0125	t_f=[5.0,8.0] t_s=[12.0,18.0] p_{23}=0.0125	t_f=[8.0,10.0] t_s=[12.0,18.0] p_{33}=0.0375	t_f=[10.0,12.0] t_s=[12.0,18.0] p_{43}=0.0375	t_f=[12.0,18.0] t_s=[12.0,20.0] p_{53}=0.0125	t_f=[12.0,18.0] t_s=[20.0,80.0] p_{63}=0.0125
[6.0,12.0] ***p*=0.25**	t_f=[0,5.0] t_s=[6.0,12.0] p_{12}=0.025	t_f=[5.0,8.0] t_s=[6.0,12.0] p_{22}=0.025	t_f=[6.0,10.0] t_s=[8.0,12.0] p_{32}=0.075	t_f=[6.0,12.0] t_s=[10.0,12.0] p_{42}=0.75	t_f=[6.0,12.0] t_s=[12.0,20.0] p_{52}=0.025	t_f=[6.0,12.0] t_s=[20.0,80.0] p_{62}=0.025
[0,6.0] ***P*=0.5**	t_f=[0,5.0] t_s=[0.0,6.0] p_{11}=0.05	t_f=[0,6.0] t_s=[5.0,8.0] p_{21}=0.05	t_f=[0,6.0] t_s=[8.0,10,0] p_{31}=0.15	t_f=[0,6.0] t_s=[10.0,12.0] p_{41}=0.15	t_f=[0,6.0] t_s=[12.0,20.0] p_{51}=0.05	t_f=[0,6.0] t_s=[20.0,80.0] p_{61}=0.05
↑ $y=f_1(t)$ $X=f_2(t)$ →	**[0,5.0]** ***p*=0.1**	**[5.0,8.0]** ***p*=0.1**	**[8.0,10.0]** ***p*=0.3**	**[10.0,12.0]** ***p*=0.3**	**[12.0,20.0]** ***p*=0.1**	**[20.0,80.0]** ***p*=0.1**

Table 1. A *joint tableau* showing discretizations of marginals $f_1(t)$, and $f_2(t)$ in bold.

2) Given two discretized input probability density functions, one for the time to failure of each component, a discretized joint density function is represented by a grid of cells, termed the *joint tableau*. Table 1 shows an example. Marginals $f_1(t)$ and $f_2(t)$ are discretized. They represent the probabilities of failure over time for components C_1, and C_2 respectively. Each marginal cell contains a time interval

[lower, upper], representing a time period during which component failure might occur, and a probability p that the component will fail during that time period. The marginal intervals shown share end points, which is not significant unless the pdf contains an impulse at a shared value, in which case overlaps can be removed by giving appropriate intervals open endpoint(s).

A discrete representation of the joint density function appears in Table 1 as the interior (non-bolded) cells. Each such cell contains a value p_{ij} for the probability assigned to the interval-valued bucket in the cell for time t_f of the *f*irst component to fail, and another bucket for time t_s of the *s*econd component (i.e. both components) to fail. Each interior cell corresponds to two marginal cells, one to its left in the leftmost column, and another below it in the bottom row.

The interval-valued bucket for t_f in any given interior cell c_{ij} represents the range of times possible for the first of two components $C_1$and C_2 to fail, given that C_1 fails within the time interval of the marginal cell to the left of c_{ij} in the left hand column, and C_2 fails within the interval of the marginal cell below c_{ij} in the bottom row. Consequently, to be binned in c_{ij}, the first of C_1 & C_2 to fail can fail as early as the *min* of c_{ij}'s two marginal interval lower bounds, and as late as the *min* of its two marginal interval upper bounds.

The time interval t_s for each interior cell c_{ij} represents the range of times possible for the *second* of the components to fail (i.e. for both components to fail), given that C_1 fails within the interval in the marginal cell to the left of c_{ij} in the left column, and C_2 fails within the interval of the marginal cell below c_{ij} in the bottom row. Consequently, if a case of failure of both is binned in c_{ij}, then the last

of C_1 & C_2 to fail can fail as early as the *max* of c_{ij}'s two marginal interval lower bounds, and as late as the *max* of its two marginal interval upper bounds.

In the joint tableau shown in Table 1, the probability p_{ij} in each interior cell c_{ij} happens to be the product of the probabilities of its marginal cells, which is consistent with *s*-independence of $f_1(t)$, and $f_2(t)$. Changing the values of the p_{ij} would express a dependency relationship situation not consistent with *s*-independence.

3) Each row and column in a joint tableau defines a constraint. For Table 1, the row and column constraints are shown in Table 2.

Row constraints	Column constraints
$0.5 = p_{11}+p_{21}+p_{31}+p_{41}+p_{51}+p_{61}$	$0.1 = p_{11}+p_{12}+p_{13}+p_{14}+p_{15}+p_{16}$
$0.25 = p_{12}+p_{22}+p_{32}+p_{42}+p_{52}+p_{62}$	$0.1 = p_{21}+p_{22}+p_{23}+p_{24}+p_{25}+p_{26}$
$0.125 = p_{13}+p_{23}+p_{33}+p_{43}+p_{53}+p_{63}$	$0.3 = p_{31}+p_{32}+p_{33}+p_{34}+p_{35}+p_{36}$
$0.063 = p_{14}+p_{24}+p_{34}+p_{44}+p_{54}+p_{64}$	$0.3 = p_{41}+p_{42}+p_{43}+p_{44}+p_{45}+p_{46}$
$0.031 = p_{15}+p_{25}+p_{35}+p_{45}+p_{55}+p_{65}$	$0.1 = p_{51}+p_{52}+p_{53}+p_{54}+p_{55}+p_{56}$
$0.031 = p_{16}+p_{26}+p_{36}+p_{46}+p_{56}+p_{66}$	$0.1 = p_{61}+p_{62}+p_{63}+p_{64}+p_{65}+p_{66}$

Table 2. Marginal constraints imposed by the discretized marginals of Table 1.

These constraints only partially determine the allocation of probability among the interior cells of the joint tableau. Thus, probability can be transferred among cells as long as these constraints remain satisfied. Any particular allocation of probability among interior cells constitutes a particular discretized joint density function. Table 1 showed one such discretized joint density function. Table 3 shows another one for the same marginals. Both are consistent with the marginal constraints summarized in Table 2.

4) The value of the left envelope at some time point *t* answers the question, "What is the maximum probability which can be cumulated up to *t*?" Computing that maximum probability involves identifying interior cells with time intervals which:

i. *end* below *t*, because the probability assignments of such cells *must* contribute to cumulation $p(t_{failure} \leq t)$, and

ii. *contain t*, because the distribution of the probabilities of a cell over its interval is not determined, and therefore it is *possible* for it all be distributed at or below *t*. Because we want to maximize the cumulation by time *t,* we must assume that extreme possibility. Knowledge that such an extreme is not possible would have to be modeled via a different, e.g. finer, discretization for the marginals.

More parsimoniously stated, interior cells with interval lower bounds $\leq t$ contribute their probabilities to the cumulation at time *t*. The shaded cells of Table 3 illustrate an example.

5) Having identified the interior cells contributing to the cumulation for a given *t*, we next find the maximum amount of probability which can be allocated among them consistently with the row and column constraints. The value of *t,* and the maximum probability found, define the coordinates of a point on the left envelope.

Finding the maximum can often be done using careful inspection to move probabilities around in a joint tableau, although linear programming on a computer is much faster. Linear programming problems maximize or minimize a linear expression, called the objective function, consistently with a set of linear constraints. The constraints here are the row and column constraints (Table 2); the objective function is the sum of the probabilities of the interior cells found in Step 4, which can contribute to the cumulation; and maximization is used to find a

point on the left envelope because that envelope describes the maximum cumulation for a given time point.

Table 3 illustrates each of these points. Table 3 shows a joint tableau with the same marginals as in Table 1, though different p_{ij}, and hence a different joint probability situation. The shaded cells contribute their probabilities to the sum that gives the value of the left envelope at time t=7. These are the cells with lower bounds ≤7 because that enables them to contribute to the objective of cumulating as much probability as possible by time t=7. To achieve that objective, we must allocate probability among the interior cells in a way which assigns as much as possible to these cells consistently with the row and column constraints (which were given in Table 2). Thus the objective function, call it z, to be maximized, e.g. by linear programming or careful inspection, is the sum of the probabilities of the shaded cells:

$$z=p_{16}+p_{26}+p_{15}+p_{25}+p_{14}+p_{24}+p_{13}+p_{23}+p_{12}+p_{22}+p_{32}+p_{42}+p_{52}+p_{62}+p_{11}+p_{21}+p_{31}+p_{41}+p_{51}+p_{61}.$$

It turns out that most of the probability can be allocated among these cells, but 0.05 cannot, and must be allocated among un-shaded interior cells. Table 3 happens to lump it into the one cell containing probability p_{33} (bolded in the table for emphasis). To see intuitively that the full probability of 1.0 cannot all be allocated within the shaded cells, observe that the probabilities in each of the two fully shaded rows of interior cells must sum to the probability of its corresponding marginal cell (i.e. 0.25 for one row, and 0.5 for the other). Similarly, the probabilities in each of the two fully shaded columns of interior cells must sum to 0.1. Therefore the entire shaded area cannot contain more probability than the

total of these four values, 0.25+0.5+0.1+0.1=0.95, leaving 0.05 to be allocated elsewhere.

[30.0,100.0] p=0.031	t_f=[0,5.0] p_{16}=0.031	t_f=[5.0,8.0] p_{26}=0	t_f=[8.0,10.0] p_{36}=0	t_f=[10.0,12.0] p_{46}=0	t_f=[12.0,20.0] p_{56}=0	t_f=[20.0,80.0] p_{66}=0
[24.0,30.0] p=0.031	t_f=[0,5.0] p_{15}=0.031	t_f=[5.0,8.0] p_{25}=0	t_f=[8.0,10.0] p_{35}=0	t_f=[10.0,12.0] p_{45}=0	t_f=[12.0,20.0] p_{55}=0	t_f=[20.0,30.0] p_{65}=0
[18.0,24.0] p=0.063	t_f=[0,5.0] p_{14}=0.038	t_f=[5.0,8.0] p_{24}=0.025	t_f=[8.0,10.0] p_{34}=0	t_f=[10.0,12.0] p_{44}=0	t_f=[12.0,20.0] p_{54}=0	t_f=[18.0,24.0] p_{64}=0
[12.0,18.0] p=0.125	t_f=[0,5.0] p_{13}=0	t_f=[5.0,8.0] p_{23}=0.075	t_f=[8.0,10.0] p_{33}=**0.05**	t_f=[10.0,12.0] p_{43}=0	t_f=[12.0,18.0] p_{53}=0	t_f=[12.0,18.0] p_{63}=0
[6.0,12.0] p=0.25	t_f=[0,5.0] p_{12}=0	t_f=[5.0,8.0] p_{22}=0	t_f=[6.0,10.0] p_{32}=0.25	t_f=[6.0,12.0] p_{42}=0	t_f=[6.0,12.0] p_{52}=0	t_f=[6.0,12.0] p_{62}=0
[0,6.0] p=0.5	t_f=[0,5.0] p_{11}=0	t_f=[0,6.0] p_{21}=0	t_f=[0,6.0] p_{31}=0	t_f=[0,6.0] p_{41}=0.3	t_f=[0,6.0] p_{51}=0.1	t_f=[0,6.0] p_{61}=0.1
↑ $y=f_1(t)$ $x=f_2(t)$ →	[0,5.0] p=0.1	[5.0,8.0] p=0.1	[8.0,10.0] p=0.3	[10.0,12.0] p=0.3	[12.0,20.0] p=0.1	[20.0,80.0] p=0.1

Table 3. A joint tableau with the same marginals as in Table 1, but different values for the p_{ij}.

6) Different points on the left envelope are derived from different sets of interior cells. Recall from Step 4 that the value of t determines which interior cells are in the set contributing to the cumulated probability at time t. Because each set defines its own objective function, and hence its own linear programming problem, linear programming is called as a subroutine each time a maximal cumulation is needed. Fortunately the discrete nature of the joint tableau limits the number of linear program solutions required. The reason is that the set of interior cells to be maximized to find $p(t_{failure} \le t)$ is the same for all values of time which fall on the same side of each interior cell interval lower bound (either greater than or less than) that t does. Because there are *rows*columns* interior cells, there are *rows*columns* different lower bounds at most; and fewer if any interior cells share the same lower bound. The lower bounds partition the time line into at most *rows*columns+1* regions, each of which defines a different

linear programming problem. The separate treatment of each region also explains the staircase shape of the envelopes (Figures 3, 4, 5).

7) Obtaining the right envelope instead of the left poses a dual problem, solved as previously described except for the following.
   i. The summed probabilities of sets of interior cells are minimized instead of maximized.
   ii. Given a value of *t,* the interior cells whose probabilities should be summed are identified by whether their interval *upper* bounds are $\leq t$, rather than their lower bounds. The upper bounds are used because if a cell's upper bound is above *t,* then its probability might not contribute to the cumulation, because its probability might be concentrated at its upper bound.

   The result is the right envelope curve, which shows the smallest possible cumulative probability for any given value of *t*. The bounding curve is an envelope which bounds from the right all distribution functions corresponding to some joint density function consistent with the row and column constraints.

2.1 *S*-Independent Marginals, and Other Specific Dependency Relationships

If the marginals are assumed to be *s*-independent, a simplification of the algorithm described earlier can provide the resulting Cdf. *S*-independence implies that the assignment of probability to each interior cell is the product of its marginal probabilities, as in Table 1. These assignments are fully determined, so there is no need for linear programming. Thus Step 3 and Step 5 above become irrelevant, and Step 6 is greatly simplified by removing the linear programming subroutine calls. The result is a numerical convolution algorithm with bounding of the effects of discretization error

(Berleant 1993). If an approximate result curve is acceptable (instead of envelopes), the class of algorithm simplifies further [7], [8], [15], [16].

The argument in the previous paragraph applies to *any fully specified dependency relationship*, not just *s*-independence. Naturally, the envelopes resulting from different dependency relationships are likely to be different, because the probabilities in the interior cells of the joint tableau will be different, reflecting the different joint density functions implied by different dependency relationships (see e.g. Figure 3 of [2]).

2.2 A Software Tool

Figure 3 of this paper shows the user interface of Statool, a tool for performing DEnv [3]. The top and middle windows each show a discretized pdf for the time to failure of one of the two components. The lower window shows result envelopes bounding the space containing the Cdf for the time to the first component failure. The button labeled "Min(x,y)" was clicked to produce the result shown, while the "Max(x,y)" button would compute envelopes for the time to failure of the second component (i.e. both components). Besides min and max computations, +, –, ÷, and × computations may be invoked by the appropriately labeled buttons. Compound expressions in +, –, ÷, × may be parsed, and then computed using the "Parsing" button. Results shown in the lower window were calculated for the case of an unknown dependency relationship between $f_1(t)$ and $f_2(t)$. Marginals $f_1(t)$ & $f_2(t)$ are from Tables 1 & 3. Numerical coordinates for the envelopes may also be plotted (Figures 4 & 5) using a popup window.

2.3 Correlation

A correlation value is a constraint on the dependency relationship, but not a full description of it because different joint density functions can yield the same correlation (Equation 1, below). Thus specifying a correlation value will typically not lead to a single Cdf for the time to failure for either the first component to fail, or for both components to fail. However, it does constitute a constraint on the set of possible joint density functions, and so will tend to yield envelopes which are closer together than they would be if correlation was unspecified. An illustration is provided by the contrast between Figures 4(b) & 4(e), and between Figures 4(d) & 4(f). Figure 4 is based on the marginals in Tables 1 & 3 as inputs representing the times to failure of components C_1 and C_2. Because DEnv determines points on envelopes using linear programming (LP) routine calls, a value for correlation must be used to define a linear constraint. That constraint then supplements the column and row constraints.

To obtain a linear correlation constraint, we start with a standard formula for correlation (Equation 1):

$$\rho = \frac{\mu_{xy} - \mu_x \mu_y}{\sqrt{\sigma_x^2 \sigma_y^2}} \qquad (1)$$

where ρ is the Pearson correlation coefficient of the marginals x & y, μ_x & μ_y are the expectations (means) of x & y, and σ_x^2 & σ_y^2 are the variances of x & y. Pearson correlation is the most common variety of correlation, and is usually meant by the term "correlation" when the variety is unstated. If ρ is known, then the only term in Equation (1) which depends on the joint density function is μ_{xy}. Solving for that term, and naming

the result E_ρ to indicate it is the expectation (of xy) derived from a particular value of correlation ρ, gives Equation (2).

$$E_\rho(\rho) = \mu_{xy} = \mu_x\mu_y + \rho\sqrt{\sigma_x^2\sigma_y^2} \qquad (2)$$

The values of the symbols on the right hand side of Equation (2) can be given directly as problem inputs if available. If not available, an estimate of the value of the right hand side of Equation (2), which can be made arbitrarily accurate by discretizing sufficiently finely, is obtained by modeling the distribution of the probability associated with each interval in the discretizations of the marginals as an impulse at its midpoint. Alternatively, the right hand side can be bounded, and expressed as an interval, making the analysis somewhat more complex, and the effects on the envelopes weaker [4]. As an example, for the marginals of Tables 1 & 3, the following values might be provided: μ_x=13.5, μ_y=9.8, σ_x^2=158.8, and σ_y^2=138.192; these were computed using midpoints as just described, e.g.,

μ_y=65*0.031+27*0.031+21*0.063+15*0.125+9*0.25+3*0.5=9.8.

Then, by Equation (2), $E_\rho(0.9)$=265.62, E_ρ (–0.9)= –1.024, E_ρ (– 0.7)=28.603, $E_\rho(0)$= 132.3, etc.

The value of μ_{xy} may also be computed from the joint density function of x & y, and thus from a joint tableau, because such a tableau is a discrete representation of a joint density function. Hence,

$$\mathbf{E}_t = \mu_{xy} = \sum_{i,j} p_{ij}\mathbf{x}_i\mathbf{y}_j \qquad (3)$$

where bolding indicates intervals, the result is named $\mathbf{E}_t$ to indicate that it is an interval for the expectation derived from a joint tableau, and $\mathbf{x}_i$ & $\mathbf{y}_j$ are the intervals in the discretized marginals corresponding to the interior cell containing probability p_{ij}. For

example, in Table 3, p_{33} has marginal intervals $\mathbf{x}_3$=[8.0,10.0] & $\mathbf{y}_3$=[12.0,18.0], and evaluating Equation (3) on all of the p_{ij} of Table 3 yields $\mathbf{E}_t$=[23.55, 160.91].

We have now computed μ_{xy} in two different ways, naming them E_ρ, and $\mathbf{E}_t$. To enforce the constraint that the joint density function, as discretized by the p_{ij} and their associated intervals, is consistent with problem input ρ, the two computations must yield consistent answers. Consistency requires that the numerical value of E_ρ must be in interval $\mathbf{E}_t$. The consistency requirement is a constraint which can augment the row and column constraints in the LP subroutine calls, consequently tending to reduce the space of feasible joint density functions. Fewer feasible joint density functions tends to reduce the range of values possible for cumulative probability of failure F at any given value of time t, tending in turn to reduce the separation between left and right envelopes.

Building on examples given in the preceding paragraphs, the joint probability scenario expressed by the p_{ij} in Table 3 is consistent with ρ=0 because $E_\rho(0)$=132.3$\in \mathbf{E}_t$=[23.55, 160.91], and also with ρ= –0.7 because $E_\rho(-0.7)$=28.603$\in \mathbf{E}_t$, but not with ρ=–0.9 because $E_\rho(-0.9)$=–1.024$\notin \mathbf{E}_t$. If ρ is specified as –0.7, the envelopes around the Cdf for the time to failure of the first component to fail are closer together than the envelopes when the problem is not constrained by a value for correlation, as a comparison of Figures 4(b) & 4(e) shows.

3 Further Comparisons

The present section explores some problem variations.

Dependency structure. If marginals are assumed to be *s*-independent, the result in principle is a specific Cdf. However, DEnv discretizes the inputs, and converts the information lost by discretization into envelopes around the output [1]. The separation of

these envelopes increases when the dependency relationship between the inputs is unspecified, because that lack of information propagates to the results. Figures 4(a) & 4(b) show the different separations for the time to the first component failure, while Figures 5(a) & 5(b) show it for the time for both components to fail.

Number of failures. Because it takes longer for both components to fail than for one to fail, Cdf F_{both} will tend to be to the right of Cdf F_{one}. A comparison of Figures 4(a) & 5(a) shows this for the case of independent marginals, while Figures 4(b) & 5(b) show it for the case of unspecified dependency between the marginals. The graphs of Figure 5 are based on values for t_s (see e.g. Tables 1 & 3), which result from the *max* operation (see Step 2 of Section 2). In contrast, the graphs for Figure 4 are based on values of t_f, resulting from the *min* operation. However the density functions whose discretizations produce the marginals used as inputs for Figures 4 & 5 are the same.

Level of discretization. Unsurprisingly, the separation of the result envelopes can be significantly affected by the coarseness of the discretization. To illustrate, we compared the results for the 6x6 discretization shown in Tables 1 & 3 with a 12x12 discretization, obtained by splitting each marginal cell interval in these tables into two smaller intervals of equal width and assigning half the probability of the original to each. A comparison between 6x6 & 12x12 discretizations is shown for *s*-independent marginals by Figures 4(a) & 4(c), and for marginals of unspecified dependency in Figures 4(b) & 4(d).

The influence of discretization level on the effectiveness of correlation values as a constraint on envelopes can be substantial. A comparison between Figures 4(e) and 4(f) illustrates that. In 4(e), derived using the 6x6 discretization condition, the correlation was

–0.7. However, under the 12x12 discretization condition, a correlation of –0.7 was inconsistent with the row and column constraints. The reason is that finer discretization typically reduces the space of possible joint density functions between marginals. The reason is that more finely discretized marginals lead to more interior cells, smaller p_{ij}, and narrower intervals for $\mathbf{x}_i\mathbf{y}_j$ (see Equation 3), in turn providing tighter control over the distribution of probabilities over intervals in the joint density functions than would occur for coarser discretizations. The consequence is a narrower interval for $\mathbf{E}_t$, and hence stronger correlation constraints, perhaps strong enough to rule out some correlation values entirely. Figure 4(f) shows the results under the 12x12 discretization condition when the correlation was specified as –0.6 instead of –0.7.

In general, finer discretization tends to provide better (narrower) envelopes. However, finer discretization increases computation time [3]. The quality of a discretization may vary not only for different numbers of histogram bars, but also for different bar widths and placements on the horizontal axis. For example, the bar widths might be equal, or equal for a logarithmically scaled horizontal axis, or chosen arbitrarily and unequally. Some of these horizontal axis partitions yield discretizations which represent the pdf more closely than others. Hall and Lawry [14] discuss such issues further.

4 Conclusion

The failure properties of 2-component systems are well understood when the dependency relationship between the individual component failures is assumed. However, such an assumption can be problematic. We show that the problem can also be analyzed when no dependency relationship is assumed between the individual component failures, and

when only the correlation is known. Results are in the form of left and right envelopes bounding all cumulative distributions consistent with the limited problem specifications. The DEnv algorithm also offers the additional benefit of accounting for the weakening of results which ensues from information loss due to discretization.

These results suggest a number of paths for further investigation. One potentially important set of questions revolves around use of partial information about the dependency relationship to narrow the envelopes. We have discussed correlation here, but the joint density function might usefully be constrained in other ways as well. One approach is to identify assumptions which capture the intent of ruling out joint density functions which are "strange," in the sense of being unlikely to occur in practice. Ruling out such density functions might enable the envelopes to be narrowed significantly.

Other open questions include extension of the technique to systems of three or more components requiring joint tableaus of three or more dimensions, decision-making applications of the results, and extensions to additional related problems.

Acknowledgements

The authors express thanks to Gerald Sheblé, and Mei-Peng Cheong for valuable discussions. Continuing work on applying these ideas to problems in the electric power field has been supported in part by the Power Systems Engineering Research Center (PSERC).

References

1. Berleant, D., "Automatically Verified Reasoning with Both Intervals and Probability Density Functions," *Interval Computations* (1993 No. 2), pp. 48-70.

2. Berleant, D. and C. Goodman-Strauss, "Bounding the Results of Arithmetic Operations on Random Variables of Unknown Dependency," *Reliable Computing* **4** (2), pp. 147-165.
3. Berleant, D., L. Xie, and J. Zhang, "Statool: a Tool for Distribution Envelope Determination (DEnv), an Interval-Based Algorithm for Arithmetic on Random Variables," *Reliable Computing* **9** (2) (2003), pp. 91-108. Software available at http://class.ee.iastate.edu/berleant/s/statool.htm.
4. Berleant, D. and J. Zhang, "Using Correlation to Improve Envelopes around Derived Distributions," *Reliable Computing*, forthcoming. Http://class.ee.iastate.edu/berleant/home/.
5. Berleant, D. and J. Zhang, "Representation and Problem Solving with the Distribution Envelope Determination (DEnv) Method," *Reliability Engineering and System Safety*, forthcoming. Http://class.ee.iastate.edu/berleant/home/.
6. Bunea, C. and T. Bedford, "The Effect of Model Uncertainty on Maintenance Optimization," *IEEE Transactions on Reliability*, **51** (4) (Dec. 2002), pp. 486-493.
7. Carreras, C. and I.D. Walker, "Interval Methods for Fault-Tree Analysis in Robotics," *IEEE Transactions on Reliability*, **50** (1) (Mar. 2001), pp. 3-11.
8. Colombo, A.G. and R.J. Jaarsma, "A Powerful Numerical Method to Combine Random Variables," *IEEE Transactions on Reliability*, **R-29** (2) (1980), pp. 126-129.
9. Cooper, J.A., S. Ferson, and L.R. Ginzburg, "Hybrid Processing of Stochastic and Subjective Uncertainty Data," *Risk Analysis* **16** (6) (1996), pp. 785-791.

10. Evans, R.A., "Point Estimates – No; Interval Estimates - Yes," *IEEE Transactions on Reliability*, **51** (3) (Sept. 2002) p. 258.

11. Ferson, S., *RAMAS Risk Calc 4.0: Risk Assessment with Uncertain Numbers*, Lewis Press, Boca Raton, 2002.

12. Ferson, S., "What Monte Carlo Cannot Do," *Human and Environmental Risk Assessment* **2** (Dec. 1996), pp. 990-1007.

13. Frank, M.J., R.B. Nelsen, and B. Schweizer, "Best-Possible Bounds for the Distribution of a Sum – a Problem of Kolmogorov," *Probability Theory and Related Fields* **74** (1987), pp. 199-211.

14. Hall, J. and J. Lawry, "Generation, Combination and Extension of Random Set Approximations to Coherent Lower and Upper Probabilities," *Reliability Engineering and System Safety*, forthcoming. Http://www.cen.bris.ac.uk/civil/staff/jwh/Publications/publications.html.

15. Ingram, G.E., E.L. Welker, and C.R. Herrmann, "Designing for Reliability Based on Probabilistic Modeling Using Remote Access Computer Systems," *Proc. 7th Reliability and Maintainability Conference, American Society of Mechanical Engineers*, 1968, pp. 492-500.

16. Kaplan, S., "On the Method of Discrete Probability Distributions in Risk and Reliability Calculations – Application to Seismic Risk Assessment," *Risk Analysis* **1** (3) (1981), pp. 189-196.

17. Nelsen, R.B., *An Introduction to Copulas*, Lecture Notes in Statistics, Vol. 139, Springer-Verlag, Heidelberg, 1999.

18. Regan, H., S. Ferson and D. Berleant, "Equivalence of Methods for Uncertainty Propagation of Real-Valued Random Variables," *International Journal of Approximate Reasoning*, forthcoming. Http://class.ee.iastate.edu/berleant/home/.
19. Vaurio, J.K., "Treatment of General Dependencies in System Fault-Tree and Risk Analysis," *IEEE Transactions on Reliability*, **51** (3) (Sept. 2002), pp. 278-287.
20. Williamson, R. and T. Downs, "Probabilistic Arithmetic I: Numerical Methods for Calculating Convolutions and Dependency Bounds," *International Journal of Approximate Reasoning* **4** (1990), pp. 89-158.
21. Zhang, T. and M. Horigome, "Availability and Reliability of System with Dependent Components and Time-Varying Failure and Repair Rates," *IEEE Transactions on Reliability*, **50** (2) (June 2001), pp. 151-158.

Author Biographies

Daniel Berleant (berleant@iastate.edu) is an Associate Professor in the Department of Electrical and Computer Engineering, Iowa State University, Ames, Iowa 50011, USA, where he has been since 1999. He received his M.S. and Ph.D. (1991) degrees from the University of Texas at Austin. Web site: class.ee.iastate.edu/berleant/home.

Jianzhong Zhang (zjz@iastate.edu) is a graduate student in the Computer Engineering program of the Department of Electrical and Computer Engineering, Iowa State University. He holds M.S. degrees in statistics from Nankai University and in Computer Engineering from Iowa State University, and has worked in industry as a software engineer. He plans to obtain his Ph.D. in December, 2004.

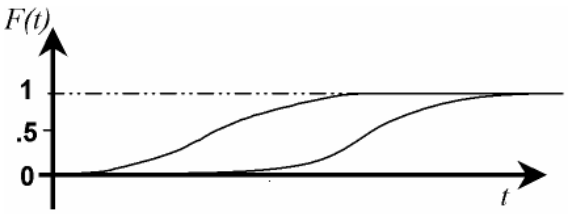

Figure 1. Left and right envelopes bounding a space of possible cumulative distributions. The *x*-axis represents time, and the cumulative probability $F(t)$ represents $p(t_{failure} \leq t)$.

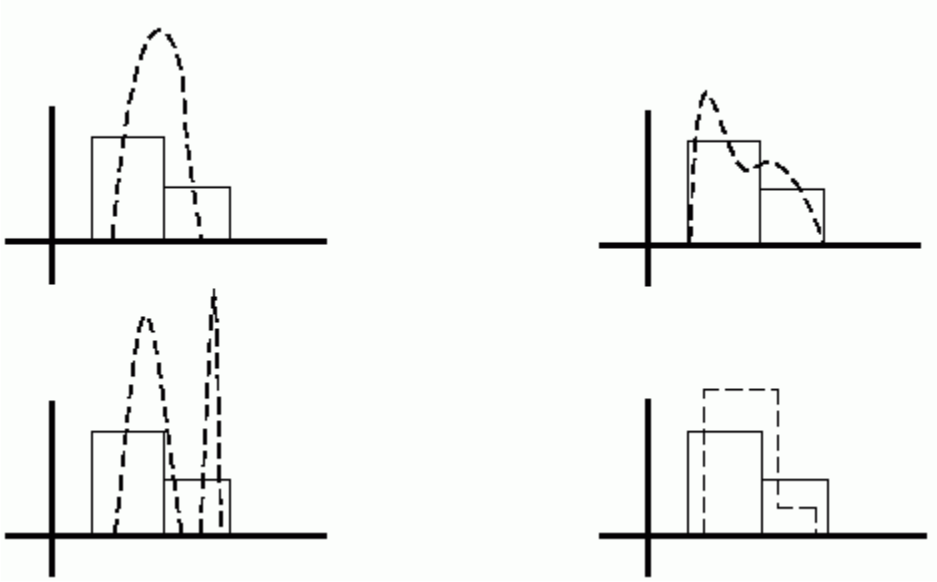

Figure 2. Four different density functions (dotted lines) and their identical discretizations as a 2-bar histogram (adapted from [1]).

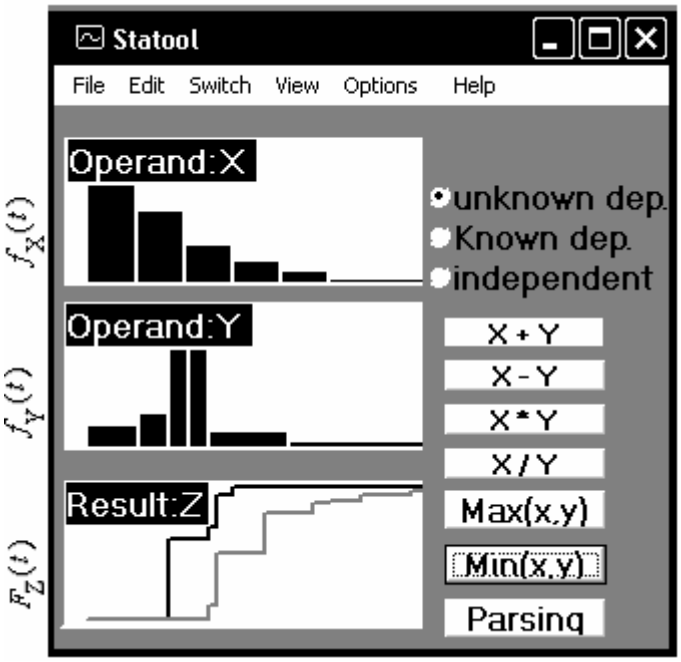

Figure 3. User interface of Statool, a software tool for performing the DEnv algorithm.

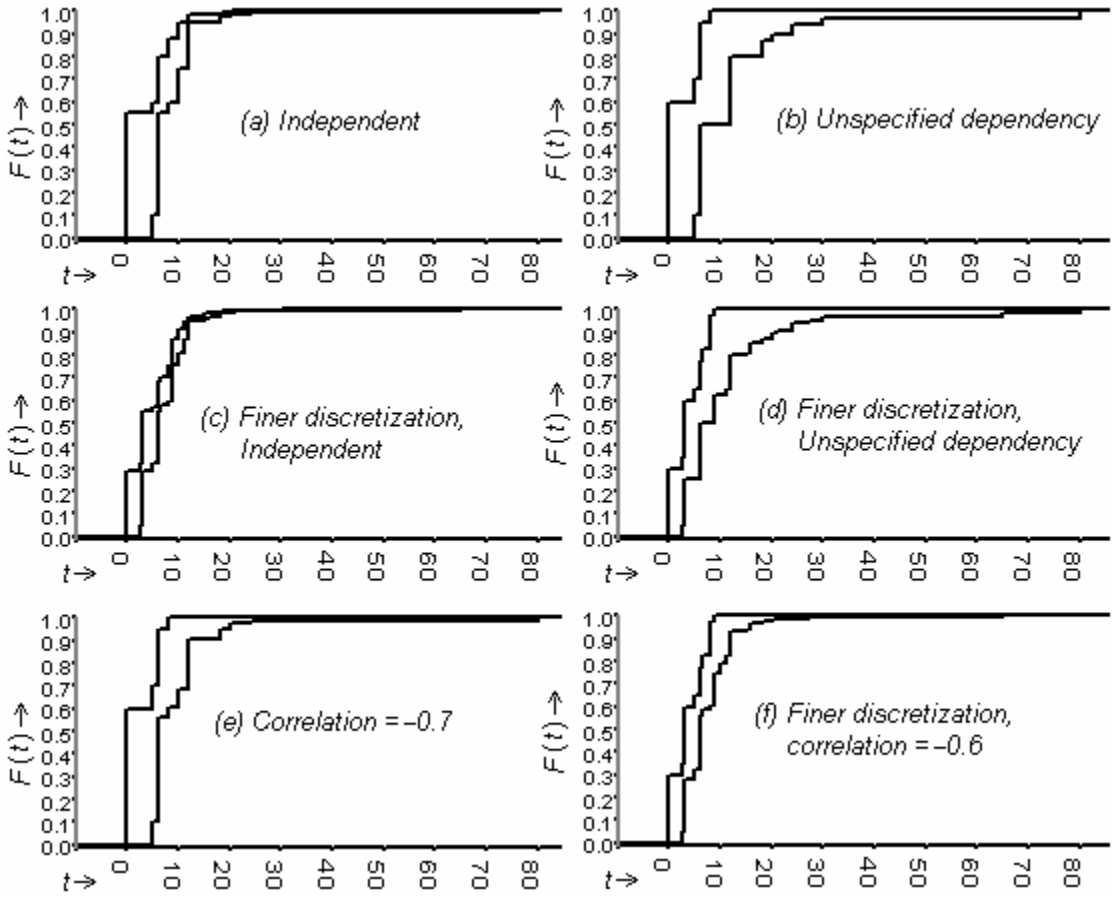

Figure 4. Bounds around the Cdf for time to first component failure under several conditions.

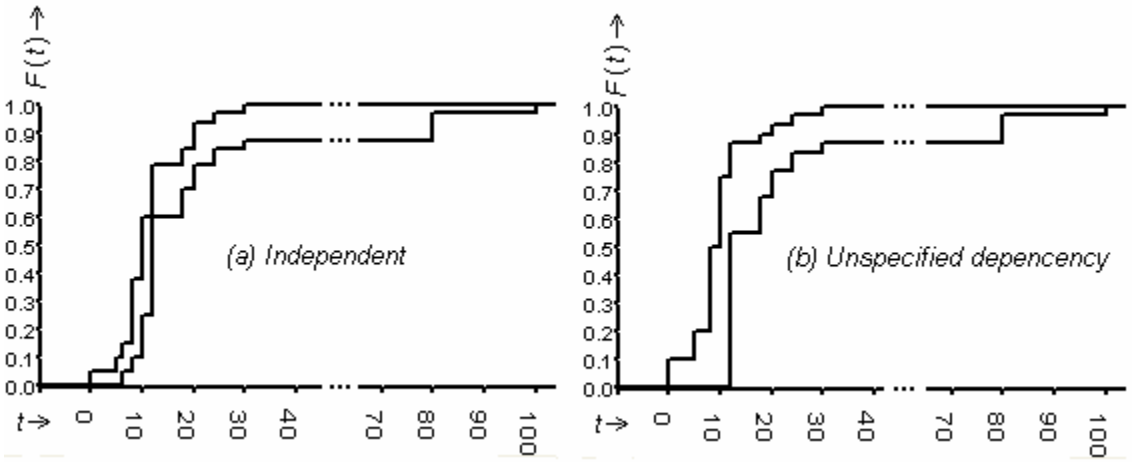

Figure 5. Bounds around the cumulative probability that *both* components will fail by time *t*.